Journal of Unconventional Oil and Gas Resources 10 (2015) 11–17

Contents lists available at ScienceDirect

Journal of Unconventional Oil and Gas Resources

journal homepage: www.elsevier.com/locate/juogr

Analysis of gas production from hydraulically fractured wells in the Haynesville Shale using scaling methods ☆

Frank Male [a,*], Akand W. Islam [a], Tad W. Patzek [b], Svetlana Ikonnikova [a], John Browning [a], Michael P. Marder [a]

[a] University of Texas at Austin, Austin, TX, USA
[b] King Abdullah University of Science and Technology, Thuwal, Saudi Arabia

ARTICLE INFO

Article history:
Received 22 December 2014
Revised 5 March 2015
Accepted 6 March 2015
Available online 21 March 2015

Keywords:
Reservoir engineering
EUR
Universal curve
PVT solver

ABSTRACT

The Haynesville Shale is one of the largest unconventional gas plays in the US. It is also one of the deepest, with wells reaching more than 10,000 ft below ground. This uncommon depth and overpressure lead to initial gas pressures of up to 12,000 psi. The reservoir temperature is also high, up to 300 °F. These pressures are uniquely high among shale gas reservoirs, and require special attention when modeling. We show that the method developed by Patzek et al. (2013) scales cumulative gas production histories of individual wells such that they all collapse onto one universal curve. Haynesville wells can take months or years for flowing tubing pressure to stabilize, so we modified the universal curve to take this delay into account. We have written a custom Pressure–Volume–Temperature (PVT) solver to calculate gas properties at the high reservoir pressure and temperature. When we apply the Patzek et al. scaling theory to 2199 individual wells in the Haynesville, we find 1546 wells have entered exponential decline due to pressure interference. We use a simple physical model to determine the time to interference, for wells with geologic parameters typical of the Haynesville, and use this time to interference to determine a field-wide stimulated permeability. Using this permeability, we arrive at an estimate of the times to interference for the remainder of Haynesville wells, and obtain production forecasts for all individual wells.

Introduction

Before the advent of horizontal drilling and hydraulic fracturing technology, the Haynesville Shale was impossible to produce. The Haynesville Formation lies at depths from 10,300 ft to 14,000 ft (Parker et al., 2009), and has a payzone thickness of only 150 ft. Since laboratory estimates for permeability obtained from shale core samples are on the order of nanodarcies (Nunn, 2012), it would be impossible to extract economic quantities of natural gas from the Haynesville Shale without horizontal wells and massive hydrofractures that open and link to natural fractures.

In addition to being deeper than all other major shale gas plays, the Haynesville is hot, with temperatures that reach above 300°F. It is abnormally pressured, with gradients of approximately 0.95 psi/ft, leading to reservoir pressures that can reach beyond 13,000 psi (Hammes et al., 2011). The Haynesville play lies in East Texas and North Louisiana, and was deposited during the Jurassic period, with the prehistoric Sabine Island at the southern boundary. There has been essentially no condensate production, and adsorption is negligible due to the high reservoir temperature.

This paper applies the methodology of Patzek et al. (2013), first applied to the Barnett Shale, to determine well decline curves and productivity for the wells drilled in the Haynesville Shale. We start by describing the underlying theory of our type curves using scaling arguments. We modify the original model to include early-time throttling of wells performed by operators using chokes, and introduce a custom PVT solver to calculate gas properties at the reservoir conditions. We fit well production to the scaling curves and use the fits to estimate the field's average stimulated permeability. Finally, we provide estimates of time to interference and ultimate recovery for producing wells. Scaling curves have been used previously to describe a great deal of physical phenomena (Abrahams et al., 1979; Rapoport, 1955; Mirzaei-Paiaman and Masihi, 2013).

We performed this work as part of a project to forecast field-wide production for the Haynesville Shale. The workflow here is similar to that in Browning et al. (2013), covering predictions for the Barnett Shale, and Browning et al. (2014), forecasting

☆ Thanks to Sloan Foundation for funding.
* Corresponding author.
E-mail address: frmale@utexas.edu (F. Male).

http://dx.doi.org/10.1016/j.juogr.2015.03.001
2213-3976/

Nomenclature

c	isothermal compressibility, 1/psi [1/Pa]
d	hydrofracture spacing half-length, ft [m]
k	permeability, md
H	height of hydrofractures, ft [m]
L	half-length of hydrofractures, ft [m]
m	real gas pseudopressure,
M	mass of gas in place, lb [kg]
N	number of fractures
p	pressure, psia [kPa]
RF	recovery factor function
S	saturation
t	time, s [s]
u	superficial flow rate ft/s [m/s]
x	distance, ft [m]
α	hydraulic diffusivity, ft^2/s [m^2/s]
ϕ	porosity
ρ	density, lb/ft^3 [kg/m^3]
μ	viscosity, cp [MPa.s]
τ	time to interference, d [s]

Subscripts

g	gas
i	initial conditions
s	scaling for throttling

Diacritics

$\sim$	scaled version of quantity

production in the Fayetteville Shale. We obtain well production histories from the IHS CERA database and the relevant geologic data from Dr. Smye's group in the Bureau of Economic Geology at the University of Texas at Austin. We then forecast production well-by-well, and use cumulative gas production to tier well acreage and build well inventories. These are then "mined" by an activity-based economic model to arrive at the full-field production forecasts.

Statement of theory and definitions

The model we use is surprisingly parsimonious. Popular numerical simulations include full 3-dimensional compositional models, and the trilinear flow model which includes finite-conductivity fractures flowing toward the wellbore and flow from outside the Stimulated Reservoir Volume (SRV), first developed by Olarewaju and Lee (1989). Because we are trying to describe the production of several thousand wells, we considered full reservoir simulators to be too unwieldy. Instead, we choose a model simpler than the trilinear flow model because the most important timescale of flow is that of gas within the SRV. Yu and Sepehrnoori (2014) show that fracture conductivity can vary by more than a factor of two without a large effect on gas production. Regarding flow from outside the SRV, we show that the permeability within the SRV is one to two orders of magnitude larger than the laboratory values obtained for unstimulated shale, making outside flow negligible.

In order to build a minimal model for natural gas flow in a hydraulically fractured well, we must start with the basic equations that govern the flow. The first is Darcy's law that relates horizontal flow in a porous medium to the gradient of pressure (Darcy, 1983):

$$u_g = \frac{k}{\mu_g}\frac{\partial p}{\partial x}, \tag{1}$$

where u_g is the superficial gas velocity, k is permeability, μ_g is the gas viscosity, and x is the distance from the hydrofracture plane.

The second equation is mass balance of the gas:

$$-\frac{\partial(\rho_g u_g)}{\partial x} = \frac{\partial}{\partial t}\left[\phi S_g \rho_g + (1-\phi)\rho_a\right], \tag{2}$$

where t denotes time, ρ_g is the gas density, ϕ is the porosity, and S_g is the gas saturation.

These equations can be generalized to three dimensions, but the simplest picture of flow near a hydrofractured well is that of a cuboid volume of stimulated rock with a uniform set of planar hydrofractures draining it. This mental model lends itself to one-dimensional analysis. Combining the two equations leads to the following partial differential equation:

$$-\frac{\partial}{\partial x}\left(\frac{k\rho_g}{\mu_g}\frac{\partial p}{\partial x}\right) \approx \phi S_g \frac{\partial \rho_g}{\partial p}\frac{\partial p}{\partial t} + (1-\phi)\frac{\partial \rho_a}{\partial \rho_g}\frac{\partial \rho_g}{\partial p}\frac{\partial p}{\partial t}. \tag{3}$$

Here we introduce the analysis of Patzek et al. (2013), who apply the Kirchhoff integral transformation of gas pressure pioneered by Al-Hussainy et al. (1966), leading to an equation based on the real gas pseudopressure, and then we introduce a set of scaling factors to build a nondimensional version of the resulting equations. The scaling factors are:

$$\mathcal{M} = (N+1)4\rho_i LHd\phi S_g \tag{4}$$

where $\mathcal{M}$ is the gas in place inside the SRV, N is the number of fractures, ρ_i is the initial density, L is the fracture half length, and H is the fracture height; and

$$\tau = d^2/\alpha_i, \tag{5}$$

where τ is the time to interfracture interference. The parameter d denotes fracture half-distance, α_i is the time at initial reservoir conditions.

Scaling laws are not unprecedented, with Rapoport (1955) performing scaling analysis to study multi-phase flow in the reservoir. Rapoport used them to assist in interpreting experimental work on oil–water flow systems, whereas we are using them to simplify a one phase flow, numerical model. The scaled transport equation is:

$$\begin{aligned} &-\frac{\partial \tilde{m}}{\partial \tilde{t}} = \frac{\alpha}{\alpha_i}\frac{\partial^2 \tilde{m}}{\partial \tilde{x}^2}, \\ &\tilde{m}(\tilde{x}, \tilde{t}=0) = \tilde{m}_i(\tilde{x}), \\ &\tilde{m}(\tilde{x}=0, \tilde{t}) = f(\tilde{t}/t_s), \\ &\partial \tilde{m}/\partial \tilde{x}|_{\tilde{x}=1} = 0, \end{aligned} \tag{6}$$

where the function of scaled real gas pseudopressure at $x = 0$ slowly varies with time to correspond to the flowing wellbore pressures experienced in a typical Haynesville well. A plot of this variation in real time is given in Fig. 1. This provides the boundary condition for the fracture face. The midpoint between fractures, $\tilde{x} = 1$, has a no-flow boundary condition. Flow is proportional to the divergence of pseudopressure, so when the divergence vanishes, there is no flow. After this system is solved numerically, the mass flow rate into the fracture can be calculated from

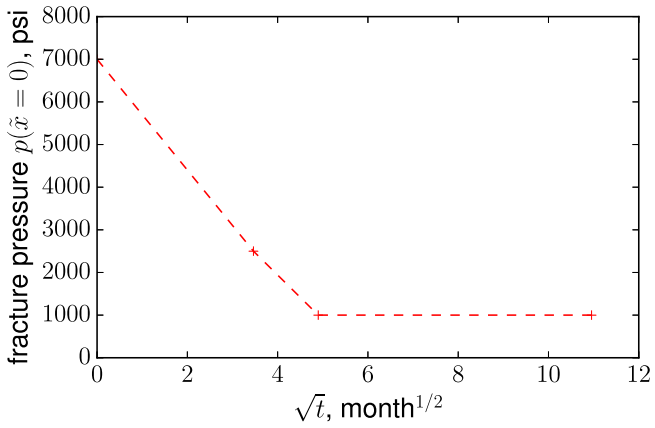

Fig. 1. Bottomhole Pressure for a typical Haynesville well.

$$\dot{\mathbf{m}} = \frac{\mathcal{M}}{\tau}\frac{\partial \tilde{m}}{\partial \tilde{x}}\bigg|_0. \tag{7}$$

Integrating this equation with respect to dimensionless time provides the cumulative production, which can be written as

$$\frac{\mathbf{m}}{\mathcal{M}} = \mathrm{RF}(\tilde{t}), \text{where} \quad \mathrm{RF}(\tilde{t}) \equiv \int_0^{\tilde{t}} d\tilde{t}' \frac{\partial \tilde{m}}{\partial \tilde{x}}|_0(\tilde{t}'), \tag{8}$$

The solution for the fractional recovery factor (RF) follows three distinct phases. During the initial period, the well is throttled, and the pressure at the fracture faces slowly varies. In this period, production rate declines slowly. After the pressure at the fracture face stabilizes, production rate declines as one over the square root of time, so that

$$\dot{\mathbf{m}} \propto \frac{1}{\sqrt{t - t_0}}$$

where t_0 varies as a function of initial pressure, p_i, and the characteristic time for choking, t_s, but is usually between 0 and 4 months. This describes production until adjacent fractures begin to interfere. After $t = \tau$, flow is boundary-dominated and the rate follows exponential decline.

Description of approach

The initial boundary value problem (6) is solved at varying initial reservoir pressures using a fully implicit numerical solver, implemented in Python.

Reservoir pressures in the Haynesville average 10,000 psi. This leads to bottomhole flowing pressures that take up to two years to stabilize as the flowing tubing pressure is slowly reduced through choke changes to the prevailing pressure of surface facilities. In order to account for this slow bottomhole pressure decline, we allow the fracture pressure to vary with time. State well tests for Haynesville wells reported that flowing tubing pressure was initially 7000 psi, dropped to 2500 psi after one year, and stabilized at 1000 psi starting at year two. We plot the presumed fracture pressure in Fig. 1. We matched the flowing tubing pressure decline curve to real well productions best with a $t_s = 0.3$, and used it for all Haynesville wells. The characteristic time for choking, t_s, results from the fact that operators must restrict flow during the early months of production to match pipeline and processing plant pressures. So long as similar facility constraints are present, we should obtain a similar production pattern should for future wells. The sensitivity of the fit to t_s is very low, because we do not fit the wells in their first four months of production while transients are most pronounced.

A further adjustment is necessary in light of the high reservoir pressures. We developed a custom PVT package consisting of the appropriate equation-of-state (EOS) and models for calculations of the thermophysical properties of natural gas mixtures. This package calculates the density (ρ), the compressibility factor (Z), the viscosity (μ), and the isothermal compressibility (c) of a natural gas mixture for given temperature, pressure, and molar fractions of gas components. As mentioned, temperatures and pressures can be very high in the Haynesville. Therefore, PVT computations cover wide ranges of temperature, 100–340°F, and pressure, 100–15,000 psi, respectively. It is observed that with appropriate mixing rules for critical properties (Sutton et al., 1985), Peng-Robinson computes density better than other models, such as that by Redlich and Kwong (1949), the Dranchuk and Abou-Kassem (1975) model, etc. Fig. 2 shows calculations of typical Haynesville gas mixtures (CH_4 95%, C_2H_6 1%, CO_2 4.8%, and N_2 0.1%) extracted from a technical report by Bullin (2008). The results shown are validated against the closest compositions data (CH_4 86.3%, C_2H_6 6.8%, C_3H_8 2.4%, n-C_4H_{10} 0.48%, iso-C_4H_{10} 0.43, C_5H_{12} 0.22%, C_6H_{14} 0.1%, C_{7+} 0.04%, and CO_2 3.2%) available in the API monograph by Gonzalez et al. (1970). While selecting the sample mixture, we gave more weight to CO_2 concentration because PVT properties of acid gases change widely, especially at high temperatures and pressures. Our package shows good agreement with experimental data. Small deviations occur at higher pressures because the compositions were not identical. Fig. 3 validates the gas viscosity data. Lee's formulae were used in the gas viscosity calculations (Lee et al., 1966). The formula from Matter and Brar (1975) was used for calculations of the isothermal compressibility of gas.

We have obtained production data and directional surveys for 2696 horizontal wells in the Haynesville from the IHS CERA database. Pay zone thickness, clay-corrected porosity, and pressure data were extracted for each individual well from the geologic model built by Smye et al. from well-log analysis. The recovery factor (RF) curves were calculated for the initial reservoir pressures ranging from 7000 psi to 14,000 psi, and interpolated in pressure for individual well pressures using the SciPy Interpolate package. We performed least-squares fits with the SciPy Optimize package, rejecting fits that lead to time to interference greater than 0.64 of the age of the well to assure that all fitted wells had shown signs of pressure interference. This value was chosen because when a well reaches a τ of 0.64, the uncertainty in the fit for τ is less than 20%, indicating the onset of interference. We have calculated time to interference for 1515 wells with this procedure.

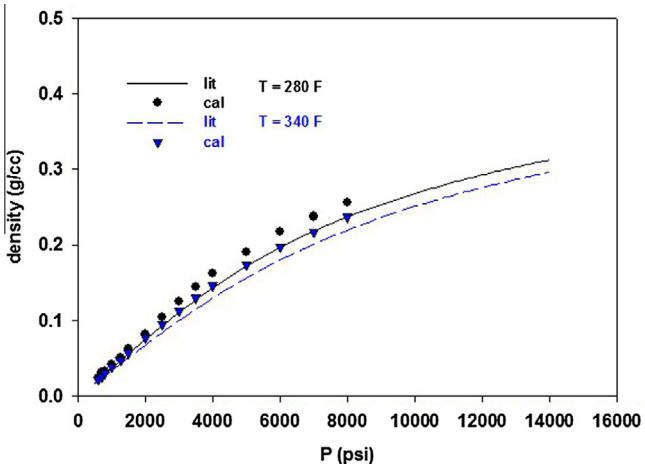

Fig. 2. Validation of density calculations (lit – literature from Gonzalez et al., 1970, cal – calculated.)

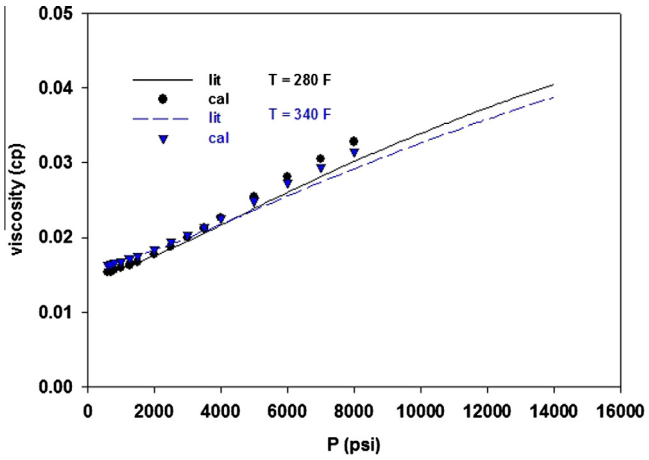

Fig. 3. Validation of viscosity calculations (lit– literature from Gonzalez et al., 1970, cal – calculated.)

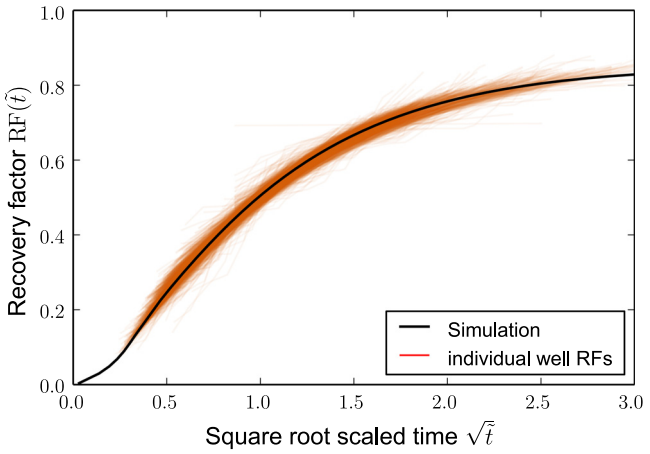

Fig. 4. Comparison of 1546 wells with scaling function. The well histories are scaled so as it fit our scaling function, which assumes an initial reservoir pressure of 10,200 psi and a well flowing pressure of 1000 psi. Each well's dimensionless time reaches 64 or more.

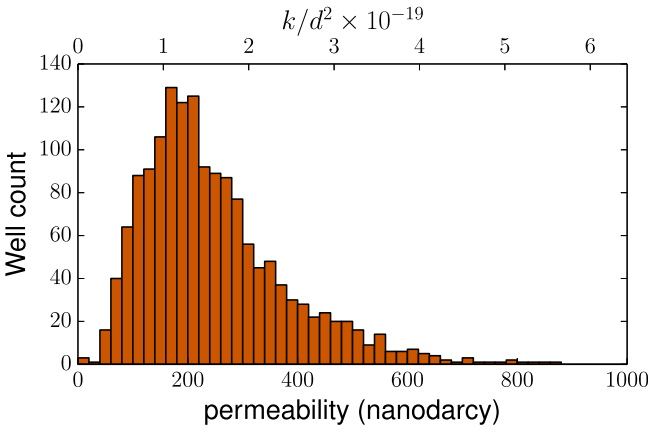

Fig. 5. Permeability values for wells that have already experienced interference, assuming 11 fracture stages. The upper axis removes that assumption and shows the values for the dimensionless parameter k/d^2.

We then estimate a field-wide average permeability by inverting the equation for the characteristic interference time, τ, matched from the individual wells. If we assume that all wells have eleven equally-spaced fracture wings, there is a field-wide average permeability of approximately 230 nanodarcy. This value is chosen as the average of the mean (250 nanodarcy) and median (218 nanodarcy) of the permeabilities determined from wells experiencing interference. The distribution of permeabilities for wells is actually rather large, as shown in Fig. 5, and choosing just one permeability from this distribution is an debatable undertaking. However, in the aggregate, selecting a conservative permeability leads to EUR estimates broadly in line with what is seen for wells that have already experienced interference.

In order to estimate τ for wells that have not shown signs of interference, we applied Eq. (5). With fluid properties at the initial reservoir pressure, a distance between hydrofracture wings of 1/11 the well horizontal length, permeability of 230 nanodarcy, and the log-derived average porosity near each well, we arrive at an estimated τ for each well. For these wells, production is fit with a set τ, and only $\mathcal{M}$ allowed to vary.

Forecasts are made for each well after their τ and $\mathcal{M}$ are established to determine their expected ultimate recovery (EUR), with production cut off at either a 25-year limit or a 0.3 MMCF/M economic limit, whichever comes first.

Presentation of data and results

We apply the model to 2199 wells that have at least 18 months of production data. Of these wells, 66 have jumps in production consistent with recompletion, and they are not forecasted. Of the remaining wells, we find that three-quarters, 1524 wells, have begun exponential decline, due to pressure interference between adjoining hydrofractures. We show the dimensionless recovery factor, RF, for the average initial reservoir pressure in Fig. 4. The Recovery Factor over time is compared directly to the set of wells that have experienced pressure interference. These wells have been offset one month in time, and fitted for cumulative production from month 4 of production until the month of July, 2013. The set had a median τ of 1.15 years, and a median 25-year EUR of 3.24 Bcf.

We can determine the effective permeability for each of these wells, given the assumed eleven equally-spaced fracture wings. We choose eleven equally-spaced stages because it has been reported as an average number for Haynesville completions. The permeability histogram is presented in Fig. 5. The median permeability for these wells is 250 nanoDarcy, but the standard deviation is large, at 147 nD, and the distribution appears to follow a log-normal distribution. This distribution has a large range, which presents some difficulty for performing time-to-interference predictions for individual wells. However, we matched the first year production to 25-year EUR distribution in order to ensure that in the aggregate these wells have accurate EUR's.

In order to forecast production for wells that have not yet exhibited interference, we must estimate either the $\mathcal{M}$ or τ for the fit. Because calculating original gas in place (OGIP) from first principles is unreliable, we estimate τ, which is only dependent upon the hydrofracture spacing and hydraulic diffusivity. We assume that all wells in the field were hydrofractured in eleven equally-spaced stages, and that these treatments created an effective permeability that was relatively constant throughout the field.

We calculate the expected time-to-interference for each well that had not yet exhibited interference to fit for $\mathcal{M}$ using the production history. From that, we make estimates of 25-year EUR's. The median EUR from this set of wells is 3.97 Bcf, and the median time to interference is 1.03 years. New completions have been designed with more stages, which might decrease d, and therefore move τ to a shorter time.

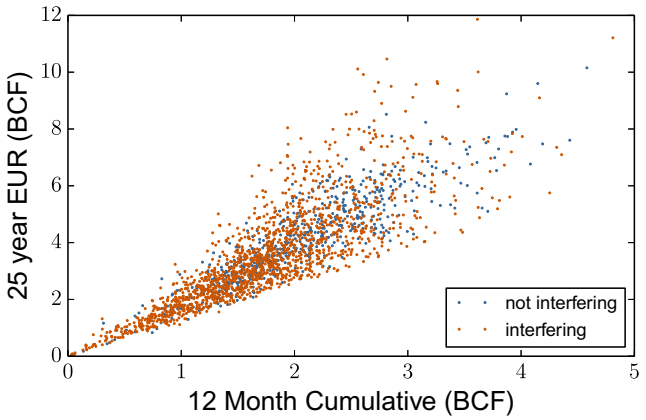

Fig. 6. Direct comparison of initial year of production to estimated ultimate recovery for all 2133 wells with at least 18 months of production history and have not been subjected to an apparent recompletion. The average well is predicted to produce 3.46 Bcf over its first 25 years, and several wells are expected to produce more than 10 Bcf.

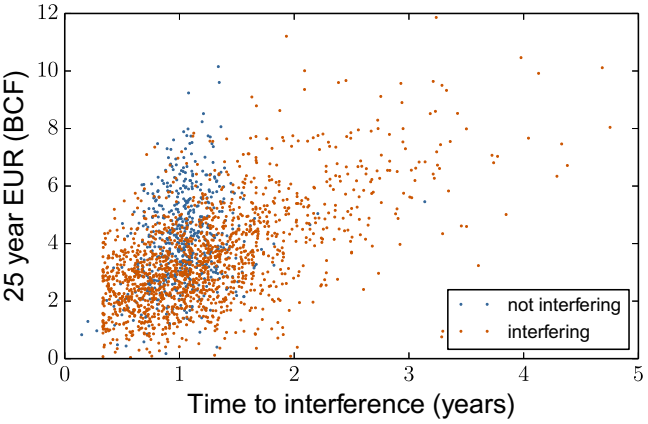

Fig. 7. Values for EUR and interference time τ for the 2133 wells in Fig. 4. The median well is expected to have an interference time of 1.06 years.

To test the fits for wells that have not yet exhibited interference, we look at the correlation between the cumulative production in the first 12 months for each well and its 25-year EUR. With an incorrect estimation of time-to-interference, the populations of already-interfering and not-yet-interfering wells diverge. Fig. 6 shows that the two are well correlated, with an R^2 of 0.725, and that the two populations completely overlap. The EUR values seem low when compared to industry expectations, but are above those predicted by Kaiser and Yu (2011), who expect the middle 40% of wells to yield EURs from 2 to 3 Bcf.

We also show the impact of fitting for τ on the EUR for each well in Fig. 7. As is evident from the scatterplot, there are many wells almost immediately switching from linear to exponential decline. In several wells, τs come close to the 4 month lower limit that we set in fitting for τ. Field-wide, the mean well interferes at 1.18 years, the median well interferes at 1.07 years. The mean and median wells, respectively, are expected to produce 3.67 Bcf and 3.44 Bcf over 25 years.

Conclusions

We have built the minimal model for fitting and predicting production from gas wells in the Haynesville Shale. The model uses a cuboid volume of hydraulically stimulated reservoir with a uniform array of hydrofractures that act as adsorbing boundaries. We assume constant effective permeability of the stimulated rock. Gas adsorption can be neglected, but the hydrofractures must have pressures that decrease over time to the final values. The timescale for pressure at the boundary to decrease was set so as to match historical production. We took care to treat the gas equation of state realistically and used a custom PVT solver to calculate the required properties natural gas mixtures, given the molar composition, pressures, and temperature found in the field. The scaling curve we used provides excellent agreement with over two thousand wells in the Haynesville Shale.

For 1,546 wells in the Haynesville, interfracture interference has set in, and we were able to determine interference time τ and gas in place $\mathcal{M}$. The typical time to interference was around 1 year. One can deduce the stimulated permeability from these wells, and we arrived at values for permeability k of roughly 240 nanodarcy. These effective permeabilities are much larger than the values found in core experiments (Nunn, 2012). EUR was estimated to be 3.24 Bcf for the median well in this set.

In order to reconcile core experiments with the observed interference, the effective hydrofracture planes would have to be much closer together. For instance, to be consistent with 10 nanodarcy permeability, the half-distance d between fractures would have to drop by a factor of five, from 200 to 40 feet. This implies that either hydrofracture stimulation leads to a series of very near-spaced hydrofractures, greatly increases permeability near the hydrofractures, or some combination thereof.

For 618 wells in the Haynesville where interference has not been observed, we used the field-wide permeability obtained from the interfering wells to estimate interference time and then fit to determine gas in place. Typical values for time to interference were 1–2 years, and EUR values were centered about 4 Bcf for this set of wells. While there is uncertainty due to the process through which we arrived at interference times for these wells, the EURs were found to correlate with initial production in the same manner as for the wells with observed interference.

As shown in Fig. 4, our minimal model of production provides an excellent fit to gas production in the Haynesville, just as it did in the Barnett. We have extended the model to include choking, and also have proposed a way to estimate ultimate recovery prior to the onset of interference. When more data become available, we will be able to make increasingly accurate forecasts, which can be used in many applications. The results of this model are used in a detailed economic analysis, which will be published elsewhere and follows the approach of Gülen et al. (2013). This work should assist policymakers in making rational decisions about the future development of gas shales, conservation of gas resources, setting minimum recovery factors in future field developments, and the economic impact of shale gas on the U.S. economy.

Acknowledgements

The production data and flowing pressure data were extracted from the IHS Cambridge Energy Research Associates database, licensed to the Bureau of Economic Geology. This paper was supported by the Shell Oil Company/University of Texas at Austin project "Physics of Hydrocarbon Recovery," with T.W.P. and M.M. as coprincipal investigators, and the Bureau of Economic Geologys Sloan Foundation-funded project "The Role of Shale Gas in the U.S. Energy Transition: Recoverable Resources, Production Rates, and Implications," with S.I. and Scott Tinker as coprinciple investigators. The work on the PVT solver was conducted with the support of the Reservoir Simulation Joint Industry Project, a consortium of operating and service companies for Petroleum and Geosystems Engineering at the University of Texas at Austin.

M.M. acknowledges partial support from the National Science Foundation Condensed Matter and Materials Theory program.

Appendix A

Here we show calculations of density, viscosity, and isothermal compressibility.

Density

Density, ρ, in g/cc is calculated from original Peng-Robinson equation of state using following correlations of critical properties (Sutton et al., 1985).

$$P_c = 756.8 - 131 \times \mathrm{SG} - 3.6 \times \mathrm{SG}^2 \tag{9}$$

$$T_c = 169.2 + 349.5 \times \mathrm{SG} - 74 \times \mathrm{SG}^2 \tag{10}$$

Here, P_c and T_c are in psi and °R, respectively. SG represents specific gravity, and is given by

$$\mathrm{SG} = \frac{1}{28.964}\sum_{i=1}^{n} y_i \times \mathrm{MW}_i \tag{11}$$

where MW_i is the molecular weight of component i, with molar fraction y_i. T_r and P_r are the reduced temperature and pressure, and are defined by the relations $T_r = T/T_c$ and $P_r = P/P_c$.

Viscosity

Viscosity μ in cp (centipoise), is computed by Lee's formula (Lee et al., 1966), which is presented as follows:

$$\mu = 10^{-4} K \exp\left(X\rho^Y\right) \tag{12}$$

where

$$X = A_1 + \frac{A_2}{T} + A_3\sum_{i=1}^{n} y_i \mathrm{MW}_i \tag{13}$$

$$K = \left(A_4 + A_5\sum_{i=1}^{n} y_i \mathrm{MW}_i\right) \times \frac{T^{1.5}}{A_6 + A_7\sum_{i=1}^{n} y_i \mathrm{MW}_i + T} \tag{14}$$

$$Y = A_8 - A_9 X \tag{15}$$

The coefficients are given by

$A_1 = 3.448$
$A_2 = 986.4$
$A_3 = 0.01009$
$A_4 = 9.379$
$A_5 = 0.01607$
$A_6 = 209.2$
$A_7 = 19.26$
$A_8 = 2.447$
$A_9 = 0.2224$

Isothermal compressibility

First compressibility factor, Z, is determined from the Peng and Robinson (1976) Equation of State. The reduced compressibility c_r is calculated from Eq. (16) where $c_r = cP_c$. Here c is in psi^{-1}.

$$c_r = \frac{1}{P_r} - \frac{0.27\frac{\partial Z}{\partial \rho_r}}{ZT_r\left(1 + \rho_r\frac{\partial Z}{\partial \rho_r}/Z\right)}, \tag{16}$$

Where

$$\frac{\partial Z}{\partial \rho_r} = B_1 + B_2\rho_r + 5B_3\frac{\rho_r^4}{T_r} + 2\rho_r\exp(-A_8\rho_r^2)\frac{B_4}{T_r^3}. \tag{17}$$

The reduced density is given by $\rho_r = \rho/\rho_c$ and $\rho_c = 0.27P_r/ZT_r$. The constants B come from the relations.

$$B_1 = A_1 + \frac{A_2}{T_r} + \frac{A_3}{T_r^3} \tag{18}$$

$$B_2 = A_4 + \frac{A_5}{T_r} \tag{19}$$

$$B_3 = A_5 \times A_6 \tag{20}$$

$$B_4 = A_7\left(1 + A_8\rho_r^2 - A_8^2\rho_r^4\right) \tag{21}$$

The necessary coefficients of Eqs. 18,21 are

$A_1 = 0.31506237$
$A_2 = -1.0467099$
$A_3 = -0.57832729$
$A_4 = 0.53530771$
$A_5 = -0.61232032$
$A_6 = -0.10488813$
$A_7 = 0.68157001$
$A_8 = 0.68446549.$

References

Abrahams, E., Anderson, P.W., Licciardello, D.C., Ramakrishnan, T.V., 1979. Scaling theory of localization: absence of quantum diffusion in two dimensions. Phys. Rev. Lett. 42 (10), 673–676.

Al-Hussainy, R., Ramey, H.J.J., Crawford, P.B., 1966. The flow of real gases through porous media. AIME Petrol Trans. 237, 624–636.

Browning, J., Tinker, S.W., Ikonnikova, S., Gülen, G., Potter, E., Fu, Q., Hovarth, S., Patzek, T.W., Male, F., Fisher, W., Roberts, F., Medlock, K., 2013. BARNETT SHALE MODEL-1: Barnett study determines full-field reserves, production forecast. Oil Gas J. 111, 62.

Browning, J., Tinker, S.W., Ikonnikova, S., Gülen, G., Potter, E., Fu, Q., Hovarth, S., Patzek, T.W., Male, F., Fisher, W., Roberts, F., 2014. Study develops Fayetteville shale reserves, production forecast. Oil Gas J. 112.

Bullin, K., 2008. Composition variety complicates processing plans for us shale gas. In: Annual Forum, Gas Processing Association, Houston, TX, October 2008.

Darcy, H., 1983. Determination of the laws of flow of water through sand. Phys. Hydrol.

Dranchuk, P.M., Abou-Kassem, H., et al., 1975. Calculation of z factors for natural gases using equations of state. J. Canadian Petrol. Technol. 14 (03).

Gonzalez, M.H., Eakin, B.E., Lee, A.L., 1970. Viscosity of Natural Gases: Monograph on API Research Project 65, American Petroleum Institute.

Gülen, G., Browning, J., Ikonnikova, S., Tinker, S.W., 2013. Well economics across ten tiers in low and high Btu (British thermal unit) areas, Barnett Shale, Texas. Energy 60, 302–315.

Hammes, U., Scott, H.H., Ewing, T.E., 2011. Geologic analysis of the upper jurassic Haynesville Shale in east Texas and west Louisiana. AAPG Bull. 95 (10), 1643–1666.

Kaiser, M.J., Yu, Y., 2011. Haynesville Shale well performance and development potential. Nat. Resour. Res. 20 (4), 217–229.

Lee, Anthony L., Gonzalez, M.H., Eakin, B.E., et al., 1966. The viscosity of natural gases. J. Petrol. Technol. 18 (8), 997–1000.

Matter, L., Brar, G.S., 1975. Compressibility of natural gases. J. Can. Petrol. Technol., 77–80

Mirzaei-Paiaman, A., Masihi, M., 2013. Scaling equations for oil/gas recovery from fractured porous media by counter-current spontaneous imbibition: from development to application. Energy Fuels 27 (8), 4662–4676.

Nunn, J.A., 2012. Burial and thermal history of the Haynesville Shale: implications for overpressure, gas generation, and natural hydrofracture. GCAGCS J. 1, 81–96.

Olarewaju, J.S., Lee, W.J., 1989. A new analytical model of finite-conductivity hydraulic fracture in a finite reservoir. *SPE Gas Technology Symposium*, Society of Petroleum Engineers.

Parker, M.A., Buller, D., Petre, J.E., Dreher, D.T., et al., 2009. Haynesville shale-petrophysical evaluation, *SPE Rocky Mountain Petroleum Technology Conference*, Society of Petroleum Engineers.

Patzek, T.W., Male, F., Marder, M., 2013. Gas production in the Barnett Shale obeys a simple scaling theory. Proc. Natl. Acad. Sci. 110 (49), 19731–19736.

Peng, D., Robinson, D.B., 1976. A new two-constant equation of state. Ind. Eng. Chem. Fundam. 15 (1), 59–64.

Rapoport, L.A. et al., 1955. Scaling laws for use in design and operation of water-oil flow models.
Redlich, O., Kwong, J.N.S., 1949. On the thermodynamics of solutions. V. An equation of state. Fugacities of gaseous solutions. Chem. Rev. 44 (1), 233–244.
Smye, K.M., Potter, E., Hovarth, S., Roberts, F., Tinker, S.W., Geological analysis of the Haynesville Shale for 'bottom up' production forecasting and resource estimation (in preparation).
Sutton, R.P., et al., 1985. Compressibility factors for high-molecular-weight reservoir gases. *SPE Annual Technical Conference and Exhibition*, Society of Petroleum Engineers.
Yu, W., Sepehrnoori, K., 2014. Sensitivity study and history matching and economic optimization for marcellus shale. *Unconventional Resources Technology Conference*, August 2014.